Polymer Chemistry

ROYAL SOCIETY OF CHEMISTRY

PAPER

View Article Online
View Journal | View Issue

Cite this: *Polym. Chem.*, 2023, **14**, 3018

Push–pull coumarin-based one-component iodonium photoinitiators for cationic nanocomposite 3D-VAT printing†

Filip Petko, [a,b] Andrzej Świeży,[a,b] Magdalena Jankowska,[a] Paweł Stalmach[a] and Joanna Ortyl *[a,b,c]

Received 1st April 2023,
Accepted 10th May 2023

DOI: 10.1039/d3py00359k

rsc.li/polymers

In this article, we described a new group of cationic photoinitiators. The influence of the arrangement of electron-donating substituents in the coumarin chromophore on their photophysical properties and photoinitiating activity is analysed. Five new coumarin-based iodonium salts exhibit two patterns of D–π-A structure – longer and shorter. They differ in the strength of the push–pull effect, which determines all properties of such compounds. Due to the intense ICT absorption band, new photoinitiators are active at 365 nm, 405 nm, and 415 nm. They exhibit excellent photoinitiating activity toward monomers such as vinyl ethers, epoxides, oxetanes, and glycidyl ethers at room temperature. However, at elevated temperatures, their activity increases dramatically. This effect is caused by the ability of coumarin salts to thermally react with monomers at elevated temperatures. Thus, the new compound exhibits photothermal initiating activity, which helps overcome scattering and shadowing problems during composite curing. Due to this phenomenon, coumarin-based iodonium salts proved to be excellent photoinitiators for nanocomposite DLP 3D-VAT printing.

Introduction

Coumarin and its derivatives are of great interest in the field of photochemistry. Due to their properties, especially their polarized structure,[1] desirable spectral properties,[2] and high photoactivity,[3] coumarin derivatives have gained interest and application in numerous research areas such as dyes for solar cells (DSSCs)[4] and optoelectronics,[5,6] fluorescent probes in materials science[7–12] and biology,[13] components of photoresponsive polymers,[14] as well as quadrupole dyes.[15] The outstanding photoreactivity has allowed coumarin to find wide photopolymerization application. Coumarin derivatives are used as photosensitizers in cationic and radical polymerization,[16] for example, to polymerize epoxy-silicones.[17] A unique feature of coumarin-containing compounds is their ability to photodimerize.[18] When a coumarin sample is illuminated at 300 nm, a reaction occurs between the double bonds of two coumarin molecules, leading to their dimerization.[19,20] This process has been used in reversible photocrosslinking of polymers, as the dimer dissociates when illuminated at a wavelength of about 250 nm.[21] However, coumarins are particularly important because they are perfect for one-component photoinitiating systems.

With the growing interest in 3D-VAT printing,[22,23] two-photon photopolymerization[24,25] and photoinduced frontal polymerization,[26–28] there is a need to find new more efficient photoinitiating systems. Common one-component photoinitiators have disadvantages, such as poor absorption properties and low reactivity toward some monomers, which limit their application.[29,30] The solution to this problem was found to be coumarin derivatives. Chromophores based on them have been used as proton abstractors in such photoinitiator types as carboxylic esters[31–33] and ketones[34] as well as in one-component photoinitiators as oximes.[35–37]

However, there has been growing interest in cationic polymerization, particularly ring-opening polymerization, observed recently. Ring-opening cationic polymerization has numerous advantages which include low polymerization shrinkage and high mechanical resistance of the resulting materials.[38] Along with this growing interest there is also an increased development of cationic photoinitiators, which are crucial for photoinitiation of this process.[39,40] The most

[a]*Department of Biotechnology and Physical Chemistry, Faculty of Chemical Engineering and Technology, Cracow University of Technology, Warszawska 24, 31-155 Kraków, Poland. E-mail: jortyl@pk.edu.pl*
[b]*Photo HiTech Ltd, Bobrzyńskiego 14, 30-348 Kraków, Poland*
[c]*Photo4Chem Ltd, Lea 114, 30-133 Kraków, Poland*

†Electronic supplementary information (ESI) available: Materials and methods, synthetic procedures, additional electrochemical data, profiles of photopolymerization, additional DSC data, and 3D-VAT printing parameters. See DOI: https://doi.org/10.1039/d3py00359k

efficient type of cationic photoinitiator is onium salts, including compounds such as phosphonium,[41] pyridinium,[42] and sulfonium salts.[43–45] Coumarin has also found application as a chromophore in such photoinitiators. There are known sulfonium and pyridinium salts that are equipped with such chromophores.[46,47] These salts show activity not only in cationic polymerization, but also in free-radical polymerization.[48]

The most active of the onium salts are halonium salts containing a hypervalent halide atom in their structure.[49] Along with the high reactivity of these compounds also goes high instability, severely limiting their applicability. Only iodonium salts with hypervalent iodine have found practical application in photopolymerization from this group of compounds.[29] However, since the 1970s when Crivello first used diaryliodonium salts as photoinitiators for cationic polymerization,[50] their structures have mostly stayed the same. This has happened because the strongly oxidizing conditions of the synthesis of these compounds severely limit the range of functional groups that can be used in the chromophore. Thus, this limited the structures used practically only to diaryliodonium salts with simple substitutions in one or both phenyl rings.[51] Such a simple structure of these compounds makes them absorb light up to 300–320 nm. This absorption range is different from the emission of commonly used light sources and forced the use of a photosensitizer.[52] This limits the application of this type of compound and makes it necessary to search for more advanced structures of iodonium salts.

However, the situation changed radically with the appearance of new methods for the synthesis of iodonium salts.[53] The last decade has seen the emergence of many new structures of iodonium salts equipped with sophisticated chromophores such as naphthalimide,[54,55] benzylidene derivatives,[56,57] BODIPY[58] or anthraquinone, and flavone.[59] Nevertheless, despite this progress, one of the first salts with a coumarin chromophore remains one of the most active solutions, absorbing to the desired range and undergoing photobleaching.[60] Thus, further work on coumarin chromophore salts could yield promising results.

Previously, the use of a 4-methyl-7methoxycoumarin derivative as a chromophore red-shifting the absorption bands of an iodonium salt was described. Due to the polarized D–π-A structure of the chromophore and the efficient ICT-type electron transition in the salt molecule, the compound shows outstanding photoinitiating properties.[61] Beside the description of the new chromophores, the effect of electron-acceptor and donor groups in the phenyl ring of these salts on their photophysical and photochemical properties has also been investigated (Fig. 1).[62]

This article presents new structures of iodonium salts equipped with coumarin chromophores with additional substituents at positions 5 and 8. These modifications affect the hypervalent iodine binding site and the properties of the final iodonium salts. Beside analysing properties such as absorption spectra, the efficiency of photolysis and photoacid generation or electrochemical properties, the photoinitiation process has also been studied in detail. As described in this paper, the compounds we prepared are perfect for nanocomposite 3D-VAT printing photoinitiators.

Joanna Ortyl

Joanna Ortyl is a Professor in the Faculty of Chemical Engineering and Technology at Cracow University of Technology (Poland). She has also been a CEO and co-owner of Photo HiTech Ltd (Cracow, Poland), which is specialized in the development and production of one component cationic photoinitiators working under visible light since 2013. She received her PhD degree in Chemistry (speciality Photochemistry) in 2012 from Cracow University of Technology. She worked as a post-doctoral researcher under Prof. Dr Thomas Jüstel at Müenster University of Applied Sciences in the Institute for Optical Technologies (Germany). She also completed a Master of Business Economics (MBE) course at Haas School of Business at the University of California, Berkeley (USA). She worked as a Visiting Professor in Prof. Jacques Lalevée's group in Institute de Science des Matériaux de Mulhouse in 2015, 2016, and 2019. Her research is always based on organic chemistry, photochemistry of small molecules as well as photochemistry of polymerization processes but is always correlated with practical application. She is an inventor with more than 30 patents; she has received more than 50 international and national awards for her research.

Experimental

Materials

The following monomers were applied to measure the kinetics of photopolymerization processes by infrared spectroscopy: 3,4-epoxycyclohexylmethyl 3,4-epoxycyclohexanecarboxylate (CADE, from Sigma Aldrich) and tri(ethylene glycol)divinyl ether (TEGDVE, from Sigma Aldrich), while for differential scanning calorimetry the following were employed: TEGDVE (thermal measurements), bis[1-ethyl(3-oxetanyl)]methyl ether (OXT-221 from Tagosei Co.) and bisphenol A diglycidyl ether (BADGE, D.E.R. 332, from Sigma Aldrich) (photo measurements). Photo-curable polymer composites were obtained from the CADE monomer and NANOPOX A 611 (7-oxabicyclo[4.1.0] heptane-3-carboxylic acid with 5.0 wt% of 20 nm SiO_2 nanoparticles, Evonik). Their structures are shown in Fig. S1,† and they were used without further purification. As a reference, two diaryliodonium salts HIP and IOD, from Lambson Ltd, were used (Fig. S1†). The IUPAC names and structures of all new coumarin-based iodonium salts and their chromophores are presented in the ESI.† The synthetic pathways that lead to the

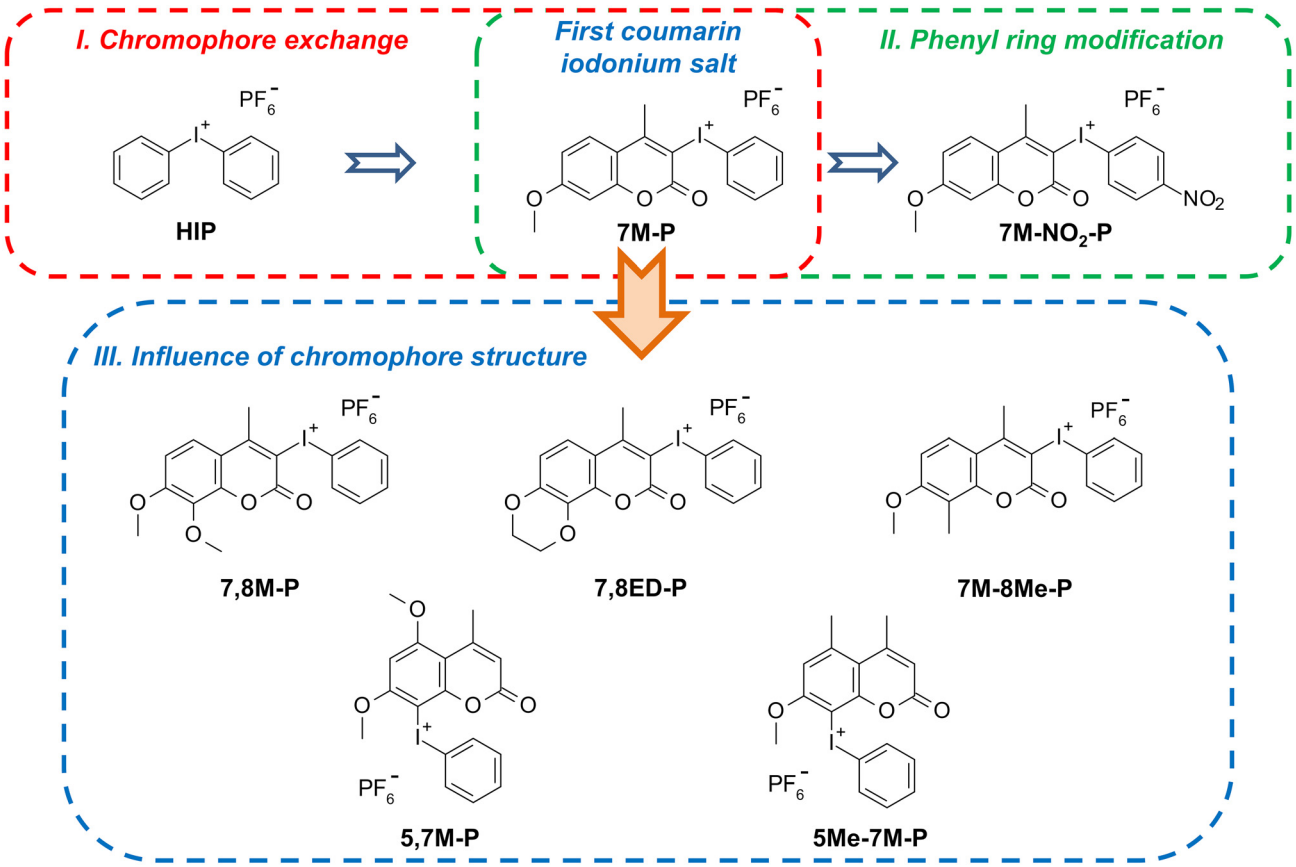

Fig. 1 Development of new coumarin iodonium photoinitiators – from chromophore exchange and phenyl ring modification to extended push–pull chromophores and the substituent impact analysis.

presented compounds and NMR and liquid chromatography–mass spectrometry (LC–MS) structural analysis results are presented in the ESI.† All reagents and solvents used during synthesis were purchased from Sigma-Aldrich, Alfa Aesar, Acros Organics, and Fluorochem and used without further purification. The reagents used in quantum efficiency measurements were purchased from Acros Organics (Rhodamine B base) and Merck (Tosylic acid monohydrate). Analytical-grade acetonitrile used in spectral, photolysis and quantum efficiency measurements was purchased from Fischer Chemicals.

Characteristics of absorption properties

UV-VIS absorption spectra of samples prepared in acetonitrile were recorded using a SilverNova TEC-X2 spectrometer (StellarNet Inc., Tampa, FL) in the range of 190–1100 nm equipped with a broadband tungsten–deuterium UV–VIS light source SL5 (StellarNet Inc., Tampa, FL). A quartz cuvette with a 1.0 cm optical path was used for measurements.

Due to the use of polychromatic light sources in the form of light emitting diodes (LEDs), there was a need to determine a value that better describes the absorption of this type of light than the molar extinction coefficient. Therefore, the amount of light emitted by the LED that is absorbed by the iodonium salt in the sample (I_a) was calculated based on spectral data and eqn (1):

$$I_a = \frac{\int_{\lambda_a}^{\lambda_b} I_0(\lambda) \cdot \left(1 - 10^{-A(\lambda)_{PI}}\right) d\lambda}{\int_{\lambda_a}^{\lambda_b} I_0(\lambda) d\lambda} \quad (1)$$

where I_0 is the normalized emission spectra of the used LED, A is the absorbance of the analysed sample, and λ is the wavelength. Values analysed in this article were calculated for a 25 μm coating containing iodonium salt at a concentration of 0.037 M as well as emission spectra of UV-LED M365L2 (λ_{max} = 365 nm) and VIS-LED M405L4 (λ_{max} = 405 nm) at the maximal power. Normalized emission spectra of all used LEDs are given in Fig. S15.†

Steady-state photolysis measurements

Photolysis of the described iodonium salts was measured in acetonitrile. 20 min irradiation of iodonium salt solutions was performed in a quartz cuvette with a 1.0 cm optical path with continuous stirring, after degassing the sample. UV-LED M365L2 (I_0 = 3.60 mW cm^{-2}), VIS-LED M405L3 (I_0 = 88.50 mW cm^{-2}), and VIS-LED M415L4 (I_0 = 117.00 mW cm^{-2}) from Thorlabs Inc. (Tampa, FL, USA) were used as light sources for sample irradiation. They were powered by a DC2200 regulated

power supply (Thorlabs Inc., Tampa, FL, USA). UV-VIS absorption spectra were obtained using the same spectrometer as for absorption measurements.

Determination of redox potentials

The redox potentials of the described compounds were determined by cyclic voltammetry measurements. They were conducted using an Electrochemical Analyzer M161 and an Electrode Stand M164 (MTM-ANKO, Poland). Tetrabutylammonium hexafluorophosphate in acetonitrile (0.1 M, Sigma-Aldrich) was used as a supporting electrolyte. A platinum disk and silver chloride (Ag/AgCl) electrode were used as the working and reference electrodes, respectively. The obtained data were recalculated and they are presented *vs.* the saturated calomel electrode (SCE) as the reference.

Determination of the quantum yield of photoacid generation

The quantum yield of acid generation was determined according to previous literature.[56,57] As a light source for irradiation, the UV-LED M340L4 (intensity I_0 = 53 mW cm^{-2}) powered by a DC2200 regulated power supply (both from Thorlabs Inc.) was used. The irradiated solutions of iodonium salts in acetonitrile were prepared so that their absorbance was 2.5 or more over the entire emission of the LED used for measurements (for absorption of nearly all incident photons). The irradiation was performed in a quartz cuvette with a 1.0 cm optical path. Samples were degassed with argon before irradiation. The dose of incident photons was small enough to photodecompose less than 5% of iodonium salt molecules. The generated acid was detected using Rhodamine B base[63] as an acid indicator and its concentration was determined using the calibration curve prepared by the gradual protonation of the solution of the Rhodamine B base in acetonitrile with *p*-toluenesulfonic acid solution. The amount of incident photons was determined using a ferrioxalate actinometer according to the IUPAC procedure.[64,65] Absorption of Rhodamine B was measured as described above.

Real time FT-IR monitoring of the progress of cationic polymerization

FT-IR measurement was performed using an FT/IR-6700 spectrometer from Jasco, equipped with an attachment dedicated to measuring photopolymerization processes. Each measurement was carried out at 25 °C. UV-LED M365L2, VIS-LED M405L3 and VIS-LED M415L4 from Thorlabs Inc. (Tampa, FL, USA) were used as light sources. The process time was 800 s; the initial 10 s of the measurement was carried out without light. The conversion of the oxirane and vinyl groups was determined based on the following equation:

$$\text{Conversion} = \left(1 - \frac{A_{\text{after polymerization}}}{A_{\text{before polymerization}}}\right) \times 100\,[\%]$$

where $A_{\text{before polymerization}}$ is the absorbance peak area characteristic of epoxy, vinyl or oxetane groups before the photopolymerization process; $A_{\text{after polymerization}}$ is the absorbance peak area characteristic of epoxy, vinyl or oxetane groups after the photopolymerization process.

Cationic photopolymerization of the epoxy monomer CADE

The reactivity of oxirane rings of the following epoxy resins was measured: 2.0 wt% of the corresponding iodonium salt and CADE. Measurements were carried out on a barium fluoride pastille. The reaction progress was monitored by the disappearance of the band characteristic of the epoxy groups (790 cm^{-1}). LEDs were employed as the light source: a λ_{max} = 365 nm diode (M365L2 Thorlabs; light intensity on the sample surface: 4.89 mW cm^{-2}); a λ_{max} = 405 nm diode (M405L3 Thorlabs; light intensity on the sample surface: 1.47 mW cm^{-2}).

Cationic photopolymerization of the vinyl monomer TEGDVE

The following polymerizing resins were prepared for kinetics measurements according to the cationic mechanism: 1.0 wt% of the corresponding iodonium salt and TEGDVE. The measurements were carried out without the presence of atmospheric oxygen, between two pieces of polypropylene foil. Vinyl group conversion was determined by the disappearance of the band located between 1570 and 1700 cm^{-1}. Measurements were carried out with UV and Vis-LEDs: λ_{max} = 365 nm diode (M365L2 Thorlabs; light intensity on the sample surface: 1.51 mW cm^{-2}), a λ_{max} = 405 nm diode (M405L3 Thorlabs; light intensity on the sample surface: 1.47 mW cm^{-2}), and a λ_{max} = 415 nm diode (M415L4 Thorlabs; light intensity on the sample surface: 7.29 mW cm^{-2}).

Hybrid cationic photopolymerization of epoxy, vinyl and oxetane groups

In addition, hybrid resins that polymerize according to the cationic mechanism were also prepared and subsequently examined for 3D printing experiments. The composition of the hybrid resins was as follows: 2.0 wt% **7M-P** and CADE/OXT-221/TEGDVE (4/3/3 w/w/w); 2.0 wt% **7M-P** and NANOPOX A 611/OXT-221/TEGDVE (4/3/3 w/w/w). A 405 nm diode (M405L3 Thorlabs; light intensity on the sample surface: 1.47 mW cm^{-2}) was applied as the light source. During the measurement, changes in the bands characteristic of epoxy (790 cm^{-1}), oxetane (980 cm^{-1}) and vinyl (1640 cm^{-1}) groups were observed in the FT-IR spectrum. The measurements were carried out on a pastille under oxygen conditions.

Photo-DSC measurements

DSC (Differential Scanning Calorimetry) measurements with a photo attachment were performed on a Photo-DSC 204 F1 Phoenix® from Netzsch-Gerätebau GmbH (Germany). The attachment dedicated to photopolymerization measurements contained 2 optical fibers, one of which exposed the test sample, while the other exposed a reference sample. The measurement system was equipped with a spot cure system Bluepoint LED eco (production by Hönle UV Technology, Germany): 365 nm diode (light intensity at the end of the fiber: 281 mW cm^{-2}); 405 nm diode (light intensity at the end of the fiber: 307 mW cm^{-2}). Light intensity was measured with

an OmniCure R2000 radiometer (produced by Excelitas Technologies, Ontario, Canada). The light source was turned on 10 s after the start of the measurement. The following compositions were prepared for photo DSC measurements: 1.0 wt% of the corresponding iodonium salt and OXT-221; 1.0 wt% of the corresponding iodonium salt and BADGE. A drop (2–2.5 mg) of each of the prepared resins was placed in an aluminum crucible and as a reference a crucible with the corresponding monomer was used (OXT-221 or BADGE). Photo-DSC measurements were carried out in an open crucible. The temperature of the measuring system for the compositions containing the oxetane monomer OXT-221 was 25 °C, while the temperature during the measurements for the monomer BADGE was 60 °C. Measurements were carried out in an atmosphere of inert gas N_2; the flow of nitrogen during photo measurements was 20 ml min^{-1}. Based on the measurements, the cationic monomer conversion (C_{DSC}) and polymerization rates (R_p) were determined. The conversion was calculated according to the following equation:

$$C_{DSC} = \frac{1}{\frac{f}{M}\Delta H_0}\int_{t_0}^{t}\frac{H(t)}{m_s}dt$$

where f – functionality of the monomer; M – molecular mass of the monomer; ΔH_0 is the enthalpy of the polymerization of the given monomer (for oxetane monomers – 107 000 J mol^{-1} and for glycidyl monomers – 80 600 J mol^{-1}); H – heat flow [W]; m_s – mass of the sample.

The polymerization rate was calculated from the formula:

$$R_p = d_i\left(\frac{H}{m_s}\right)\frac{1}{\Delta H_0}$$

where d_i – density of composition [g ml^{-1}]; H – heat flow [W]; m_s – sample mass [g]; ΔH_0 – enthalpy of polymerization [J mol^{-1}] (calculated in one functional group).

DSC measurements

Thermal measurements were performed with DSC technology. For this purpose, a DSC 204 F1 Phoenix® from Netzsch-Gerätebau GmbH (Germany) equipped with a special attachment dedicated to thermal measurements was employed. For thermal measurements, the following compositions were prepared: 1.0 wt% of the corresponding iodonium salt and TEGDVE. The neat TEGDVE monomer was used as a reference. The measurements were carried out in a closed crucible (aluminum lid pierced). In the next stage of the study, the thermal behavior of the iodonium salts was also checked. An empty crucible was used as a reference for these tests. Thermal measurements of the neat iodonium salt (without the added monomer) consisted of heating the powder in a closed crucible to 200 °C (the heating time was 90 minutes) and then cooling the measurement system to 20 °C. Thermal measurements of the composition consisting of the initiator and vinyl monomer TEGDVE consisted of heating the system to 120 °C for 50 minutes, followed by cooling to 20 °C for 10 minutes. Measurements were carried out in an atmosphere of inert gas N_2; the flow of nitrogen during thermal measurements was 50 ml min^{-1}.

Determination of 3D printing parameters and 3D printing experiments with digital light processing technology (DLP)

The determination of the optimal 3D printing parameters was to set the critical energy E_c and the depth of light penetration D_p. For this purpose, the following formula was applied:[66,67]

$$C_d = D_p \ln\left[\frac{E_0}{E_c}\right]$$

where C_d – thickness of the cured resin layer [μm]; E_0 – light energy at the surface [mJ cm^{-2}].

The critical energy (the point of intersection of the graph with the X-axis) and the light penetration depth (the slope of the obtained curve) were determined based on the $C_d = f(E_0)$ diagram. A Lumen X+™ 3D printer was employed to obtain 3D prints (the intensity of light applied to the cured resin was 9.95 mW cm^{-2}). The 3D designs to be printed were properly prepared using Fusion360® software (from AutoDesk). The following photo-curable resins were prepared for the 3D printing experiments: 2.0 wt% **7M-P** and CADE/OXT-221/TEGDVE (4/3/3 w/w/w); 2.0 wt% **7M-P** and NANOPOX A 611/OXT-221/TEGDVE (4/3/3 w/w/w).

Visual analysis of the obtained three-dimensional objects

An OLYMPUS DSX1000 optical microscope was deployed to obtain the images of the 3D obtained objects.

Results

New iodonium salt design

Coumarin has a very favourable arrangement of functional groups in the structure, which guarantees the desired photophysical and photochemical properties.[68] The ester group located in the core of coumarin ensures the proper polarity of the molecule even without additional substitutions. It is because the ester group behaves as an electron-acceptor at the double bond while slightly electron-donating at the aryl ring.[69] Thus, the coumarin core has a D–π-A structure (a conjugated bond system ensured by a styryl core), providing a push–pull effect. In the absorption spectrum of such molecules, an intense band appears at the longer wavelengths, corresponding to the intramolecular charge transfer (ICT) transition.[70]

The coumarin molecule can be more polarized by modifying it with additional electron-donating groups in the aryl ring. Such modification improves its absorption properties by red-shifting the ICT band further towards longer wavelengths. This approach led to 4-methyl-7methoxycoumarin, which was successfully used as a chromophore in the iodonium salt structure, ensuring the outstanding photochemical activity of this compound.[61] Therefore, it is possible to improve absorption properties by further using other methoxy groups ($\sigma_p = -0.27$) or weaker methyl groups ($\sigma_p = -0.17$) in appropriate positions at the aryl ring.[69]

To investigate the influence of electron-donating substituents at the aryl ring in the coumarin structure on iodonium salt properties, we prepared a group of five new coumarin-based iodonium salts (Fig. 1, blue frame). Each chromophore differs in the type and arrangement of substituents.

Theoretically, the more donating group at one side of the molecule should have improved the spectral, electrochemical, and photoinitiating properties of iodonium salts by increasing molecule polarization. However, some modifications have an undesired impact. Methyl and methoxy groups at positions 5 and 7 activate the aryl ring too strong, and hypervalent iodine binds to position 8, which was too low activated in other derivatives to undergo electrophilic substitution during iodonium salt synthesis. Therefore, in the case of **5,7M-P** and **5Me-7M-P** derivatives, the hypervalent iodine is located at 8 position instead of 3. Such substitution shortens the distance between the donor groups and the strong acceptor, hypervalent iodine. This reduces the molecule's polarity and increases its excitation energy (Fig. 2).

All presented iodonium salts were equipped with the hexafluorophosphate anion (PF_6^-). This anion generates a superacid during photolysis, which is strong enough to initiate ring-opening cationic polymerization[71,72] efficiently and is also low toxic.[73] The same anion in all derivatives allows focusing on the impact of the chromophore structure on the photoinitiation process.

Absorption properties

All the prepared coumarin-based iodonium salts have better absorption properties than simple diaryliodonium salts **HIP** and **IOD** (Fig. 3A). They absorb at longer wavelengths, which is caused by a coumarin chromophore. However, there is a differ-

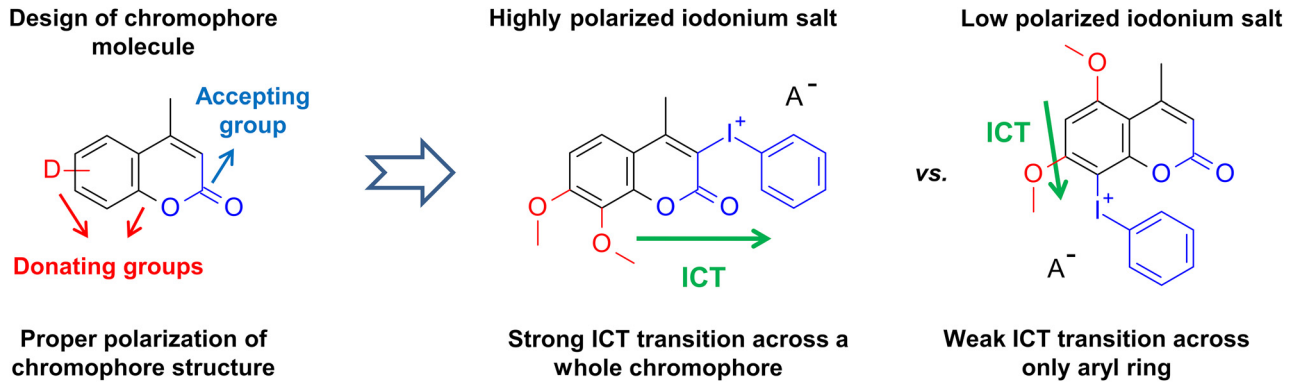

Fig. 2 Design of new iodonium salts equipped with modified coumarin chromophores. Red – electron-donating groups, black – π-bond system, and blue – electron-accepting groups.

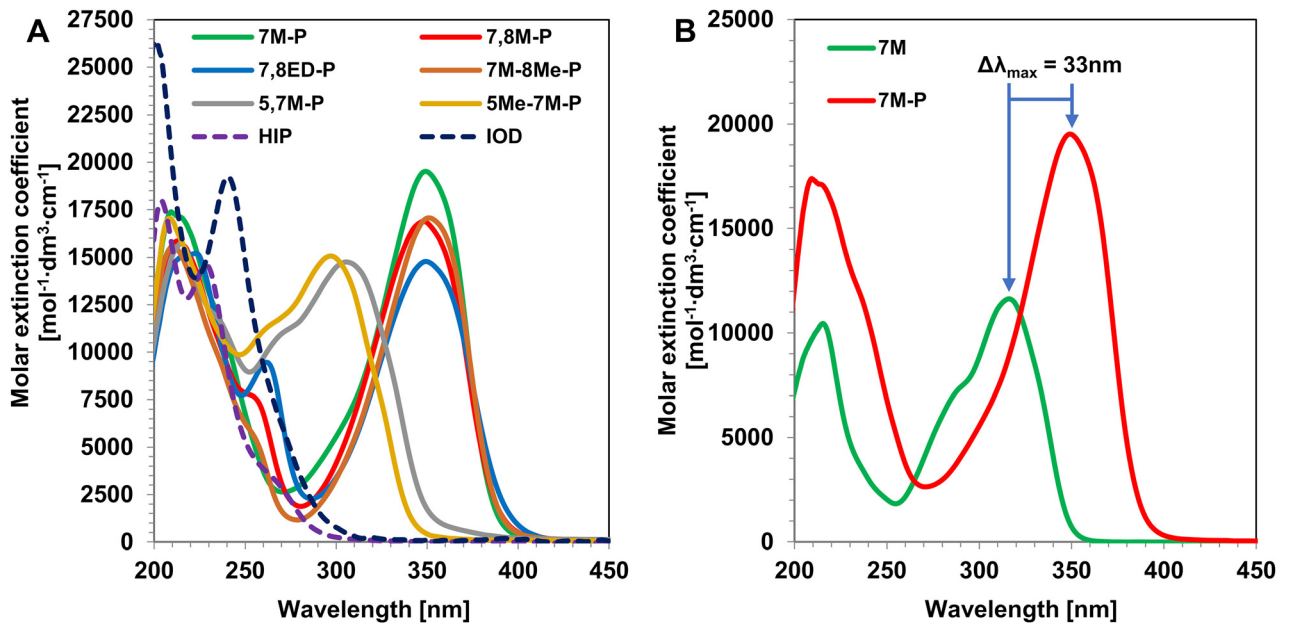

Fig. 3 Absorption spectra of the new coumarin based iodonium salts in the UV–VIS region measured in acetonitrile: (A) spectra comparison of new salts and diaryliodonium counterparts; (B) comparison of **7M-P** salts with its chromophore.

ence in the band location between **5,7M-P** and **5Me-7M-P** derivatives and the rest of the compounds. When hypervalent iodine is located at a double bond (position 3), the strong electron-accepting character of this substituent highly polarized salt structure strengthens the push–pull effect. As a result, the intense bathochromic shift is observed between **7M-P**, **7,8M-P**, **7,8ED-P**, **7M-8Me-P** and their chromophores (Fig. 3B and Fig. S16–S19†). The effect overwhelmed the impact of substituents at the aryl ring; thus, all position three derivatives have nearly the same absorption characteristics (λ_{max} between 348 and 350 nm) and the effects of methoxy and methyl groups are unobservable (Table 1).

On the other hand, hypervalent iodine at position 8 has no such significant impact. This is caused by lower polarization of the salt molecule and near donating group locations. In the case of derivatives **5,7M-P** and **5Me-7M-P** the impact of substituents is visible, exchanging the methoxy group with a weaker donating methyl group leading to absorption at shorter wavelengths (305 nm compared to 297 nm for **5,7M-P** and **5Me-7M-P** respectively). Also, the close location of the donating group neglected the polarizing effect of hypervalent iodine. There is no bathochromic shift between derivatives **5,7M-P** and **5Me-7M-P** and their chromophores. Moreover, the hypsochromic shift is observed, which is undesirable because it moves absorption away from the visible range and prevents the photobleaching of salt (Fig. S20 and S21†).

Slight differences in absorption spectra can be more noticeable when considering the amount of emitted light absorbed by the salt in the sample (I_a values, Table 1). This value better describes the absorption of polychromatic light than the commonly used molar extinction coefficient (ε). Hypothetical 25 μm thick coatings containing iodonium salts in 37 mM concentration can absorb light differently, especially at longer wavelengths. Diaryliodonium salts cannot absorb light in all three investigated ranges where their coumarin counterparts exhibit absorption. The light emitted by LED@365 nm is effectively absorbed by all four entire push–pull derivatives (**7M-P**, **7,8M-P**, **7,8ED-P**, **7M-8Me-P**). In their case, the differences in $I_{a\ 365}$ are negligible, but they absorb the light emitted by LED@405 nm and LED@415 nm noticeably differently. The salt **7,8ED-P** absorbs at the longest wavelength of all coumarin salts (Fig. 3A); therefore, it absorbs nearly two times more light emitted by both LED@405 nm and LED@415 nm in comparison with essential **7M-P** salt. A similar situation is observed in the case of **7,8M-P** and **7M-8Me-P** where two electro-donating substituents are located at 7 and 8 positions. Such a substitution causes a slight broadening of the absorption band, which results in higher absorption at longer wavelengths. These slight differences in absorption bands can have a crucial impact on the photoinitiation of the polymerization process, which strongly depends on the absorption of the used photoinitiating system.

On the other hand, coumarin iodonium salts with substituents at positions 5 and 7 (**5,7M-P** and **5Me-7M-P**) exhibit much lower absorption of light emitted by the used LED. The effect is caused by their worse absorption at longer wavelengths than the rest of the coumarin salts. Derivative **5,7M-P** with two more donating methoxy groups absorbs significantly further than **5Me-7M-P**. This is manifested in 3 times higher light absorption from LED@365 nm and 4% at LED@365 nm compared to no absorption of **5Me-7M-P**. However, both salts have negligibly low absorption compared to the entire push–pull derivatives. These effects impact the photoinitiating activity of the investigated iodonium salts and determine the rest of the results.

Steady-state photolysis experiment

All six investigated coumarin-based iodonium salts' ability to effectively photolysis under the used LEDs was studied. Samples of salts in acetonitrile were irradiated for 20 min with an appropriate LED, and the changes in the UV-VIS absorption spectrum were recorded (Fig. 4 and Fig. S22–S26†). According to the obtained results, strong push–pull salts **7M-P**, **7,8M-P**, **7,8ED-P**, and **7M-8Me-P** photolyzed in the same way under irradiation with all three used LEDs (example in Fig. 4). Due to the bathochromic shift between salt and the chromophore, these coumarin-based iodonium salts can be photobleached. Photodecomposition product spectra look similar to the absorption spectrum of the chromophore itself. Therefore, according to the proposed mechanism, we suggest that the presented iodonium salts photolysed with either simple chromophores or with the iodochromophore.[61,62] Further photochemical reactions are unlikely because the spectra clearly show isosbestic points.

In the case of the other two derivatives **5,7M-P** and **5Me-7M-P**, with shorter D–π-A structures, there were no significant

Table 1 Comparison of absorption properties, quantum yields, and reduction potentials of the presented coumarin iodonium salts and diaryliodonium counterparts

Iodonium salt	λ_{max} [nm]	ε_{max} [mol^{-1} dm^3 cm^{-1}]	ε_{365} [mol^{-1} dm^3 cm^{-1}]	$I_{a\ 365}$	ε_{405} [mol^{-1} dm^3 cm^{-1}]	$I_{a\ 405}$	ε_{415} [mol^{-1} dm^3 cm^{-1}]	$I_{a\ 415}$	Φ_{acid}	E_{red} *vs.* SCE [mV]
HIP	228	14 600	0	0%	0	0%	0	0%	n.d.	−680
IOD	241	19 230	0	0%	0	0%	0	0%	n.d.	−725
7M-P	349	19 500	15 710	84.34%	186	7.74%	80	3.65%	9.97%	−534
7,8M-P	348	16 880	13 300	82.74%	280	10.08%	100	4.61%	8.45%	−528
7,8ED-P	349	14 780	12 520	84.67%	505	14.74%	175	6.43%	7.26%	−522
7M-8Me-P	350	17 060	14 540	84.85%	210	10.42%	50	5.55%	4.72%	−576
5,7M-P	305	14 750	615	12.82%	40	4.14%	0	0%	n.d.	−646
5Me-7M-P	297	15 070	130	3.72%	0	0%	0	0%	n.d.	−624

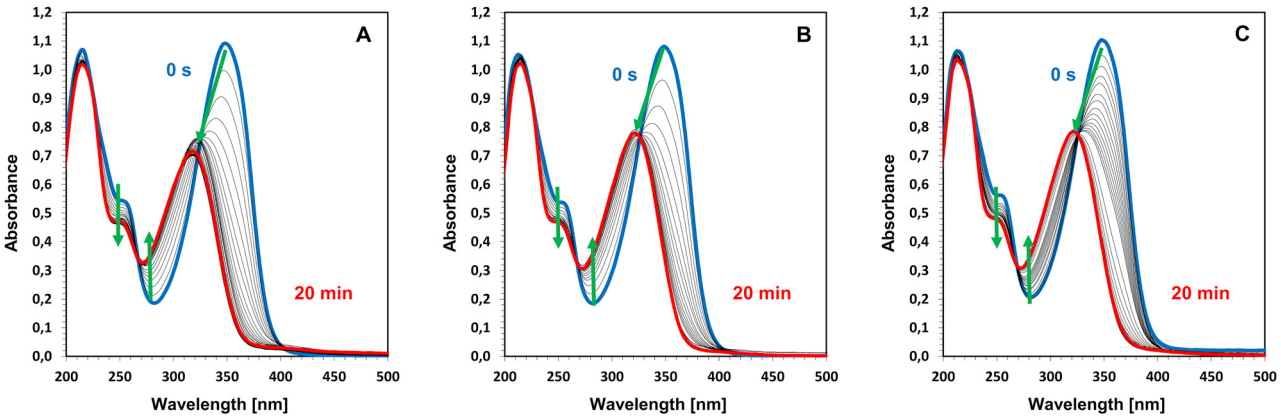

Fig. 4 Photolysis of **7,8M-P** iodonium salts measured in acetonitrile upon exposure to: (A) LED@365 nm, (B) LED@405 nm, and (C) LED@415 nm.

changes in absorption spectra during irradiation with all used LEDs (Fig. S25 and S26†). The lack of changes is not surprising under irradiation with LED@405 nm and LED@415 nm, because both compounds absorb slightly or do not absorb at all, so the photolysis of salts was not expected. However, both compounds absorb enough light to undergo photolysis under irradiation with LED@365 nm. The results indicated that both salts must be significantly more photostable than derivatives with hypervalent iodine located at the double bond. This effect may be due to the close presence of electron-donating groups in the vicinity of the C–I bond undergoing photocleavage instead of the vicinity of the withdrawing ester group in the more photo-unstable derivatives. It is known that the vicinity of donating groups can increase the chemical bond energy. In the case of iodonium salts, the energy of the C–I bond can increase by about 25% in the near alkyl group.[62] So, the effect caused by methoxy groups should be even higher. An opposite effect occurs in the presence of a withdrawing group like the ester group, the energy of C–I decreased. Therefore, derivatives with hypervalent iodine at position 3 more easily photolyzed.

Redox properties

The impact of the substituent arrangement in the chromophore structure on the electrochemical properties of coumarin-based iodonium salts was also investigated. The obtained reduction potentials are given in Table 1 and compared with common diaryliodonium salts **HIP** and **IOD**. Since hypervalent iodine is reduced in iodonium salts, its location and surroundings significantly impact the reduction potential. The acceptor environment around iodine benefits the reduction potential (increases its value) because it lowers the electron density within this group, facilitating the electron transfer from the reducer. The opposite situation occurs when there are donor groups in the vicinity. They hinder the reduction process by increasing the electron density within the hypervalent iodine bonds, significantly lowering the reduction potential. Therefore, all coumarin iodonium salts exhibit higher reduction potential than the diaryliodonium counterparts (E_{red} between −522 and −646 mV *vs.* −680 and −725 mV, respectively). The coumarin derivatives with hypervalent iodine at 3 position have the highest Ered, which increases with increased polarization of the salt structure. In this case, a higher amount of donating groups positively impacts electrochemical properties. On the other hand, such a positive effect was not observed in the case of derivatives with hypervalent iodine at 8 position in the direct vicinity of electron-donating methoxy and methyl groups. Compounds **5,7M-P** and **5Me-7M-P** behave typically. The more donating methoxy substituent lowers the E_{red} value (**5,7M-P**) in comparison with a methyl group in **5Me-7M-P.** The polarization has no significant impact because the D–π-A structure in both salts is short and limited almost to the aryl ring in the coumarin structure (Fig. 2). In conclusion, iodonium salts with a coumarin chromophore can be more easily reduced than diaryliodonium salts. Thus, the developed compounds are better suited as oxidants in two-component initiating systems used in classical photopolymerization[74] as well as in photoinduced frontal polymerization.[75]

Quantum yield of photoacid generation

During photolysis, iodonium salts release the super acid, which initiates ring-opening cationic polymerization. However, not all absorbed photons are converted into acid molecules because of relaxation processes that occur in the excited molecule. The quantum yield of photoacid generation (Φ_{acid}) indicates how effective iodonium salt can convert light energy into acid molecules. It is the second most crucial property of photoinitiators determining how efficient the photoinitiation process will be. Iodonium salts with higher Φ_{acid} need less irradiation time to initiate the polymerization process.

The Φ_{acid} values were measured and compared only for **7M-P**, **7,8M-P**, **7,8ED-P**, and **7M-8Me-P** derivatives (Table 1). The used Φ_{acid} determination method requires sample absorption in all emission ranges of the used LEDs. The LED@340 nm was used as a light source, and only the four iodonium salts with the best absorption properties fit this requirement. Compound **7M-P** is the most efficient acid generator (Φ_{acid} = ~10%), and the values for the rest of the com-

pounds decrease in the order **7,8M-P**, **7,8ED-P**, and **7M-8Me-P** to 4,7% for the least efficient salt. These results suggest that a higher number of substituents is undesirable because each additional substituent can increase the internal conversion efficiency. However, the obtained results do not indicate the direct regularity in the impact of substituents on Φ_{acid} values. Nevertheless, based on absorption properties and Φ_{acid} values three compounds **7M-P**, **7,8M-P** and **7,8ED-P** were the most promising for application as photoinitiators.

FT-IR measurements of the photoinitiating cationic polymerization activity of coumarin based iodonium salts

The photoinitiating efficiency investigation was divided into 2 stages. The first was to check the possibility of photoinitiating the cationic polymerization of the epoxy monomer CADE (Fig. 5). The second step was to check the suitability of coumarin derivatives for photoinitiating cationic photopolymerization of vinyl monomers (Fig. 6). The cationic resins were measured using UV-LED@365 nm, VIS-LED@405 nm, and VIS-LED@415 nm as light sources. The photoinitiating activity was evaluated based on 3 parameters: cationic monomer conversion, induction time, and the slope curve of the kinetic profile, which tells about the speed of the photopolymerization process.

All coumarin-based iodonium salts exhibit activity under irradiation with UV-LED@365 nm and VIS-LED@405 nm toward the CADE monomer, where simple diaryliodonium salt **IOD** remains inactive (Fig. 5 and Table 2). Absorption properties determine this activity. An intense ICT band of coumarin salts guaranteed absorption at longer wavelengths and

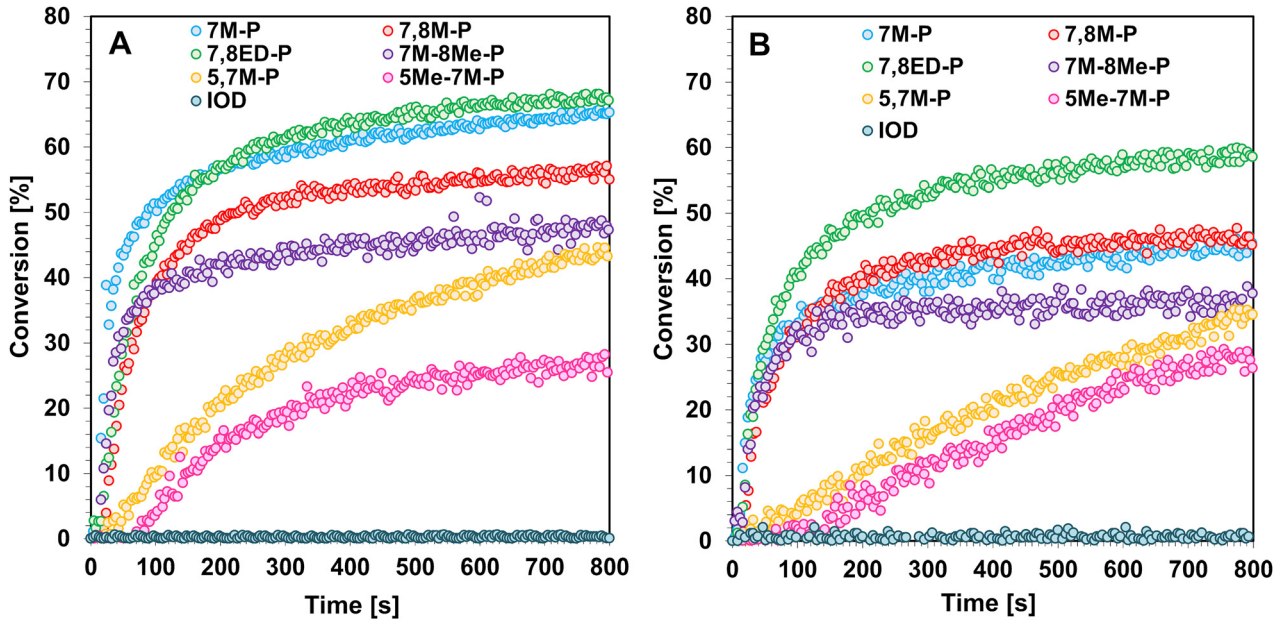

Fig. 5 Photopolymerization profiles of a 25 μm thick coating consisting of the CADE monomer and studied coumarin iodonium salts under (A) LED@365 nm and (B) LED@405 nm exposure.

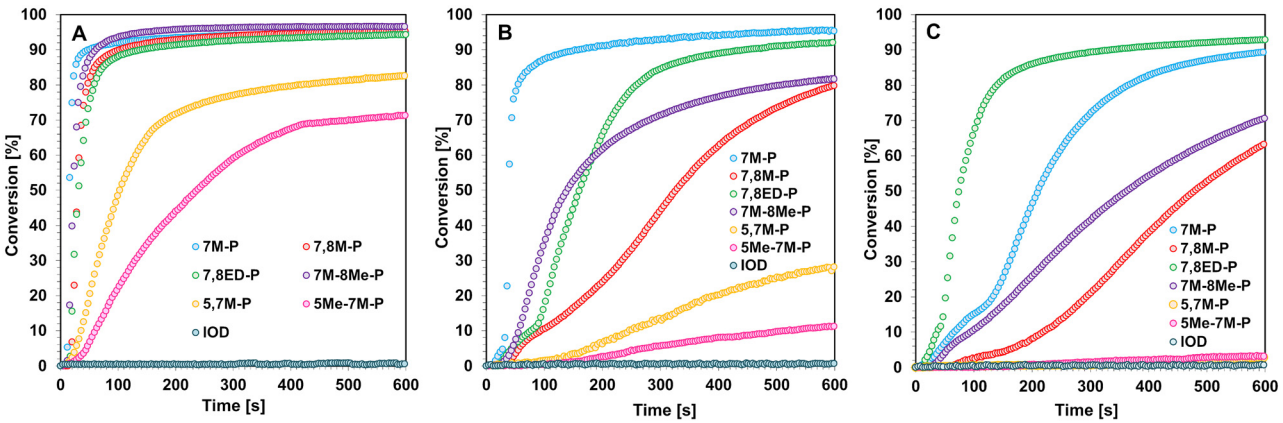

Fig. 6 Photopolymerization profiles of a 25 μm thick coating consisting of the TEGDVE monomer and studied coumarin iodonium salts under (A) LED@365 nm, (B) LED@405 nm, and (C) LED@415 nm exposure.

Table 2 Coumarin based iodonium salt photoinitiating activity parameters of CADE polymerization

	LED@365nm[a]			LED@405nm[b]		
Iodonium salt	FC [%]	τ_{ind} [s]	dC/dt	FC [%]	τ_{ind} [s]	dC/dt
IOD	—	—	—	—	—	—
7M-P	65	2.68	2.93	45	3.15	1.12
7,8M-P	56	5.40	1.02	46	6.14	1.09
7,8ED-P	68	4.25	1.16	59	4.37	1.20
7M-8Me-P	48	2.09	1.23	38	6.34	1.03
5,7M-P	45	17.46	0.14	35	20.44	0.09
5Me-7M-P	26	58.12	0.13	25	69.51	0.07

[a] I_0 = 4.89 mW cm^{-2}. [b] I_0 = 1.47 mW cm^{-2}. FC – final conversion. τ_{ind} – induction time.

allowed them photoinitiated polymerization. However, coumarin derivatives cannot cause photoinitiated CADE polymerization under VIS-LED@415 nm irradiation. The absorption of salts in this region is too low for an efficient CADE monomer whose secondary oxonium ion is stabilized by hydrogen bonds.[23]

Although all coumarin derivatives are active toward CADE, the differences in activity resulting from their absorption properties and structure can be observed. Derivatives with a long D–π-A structure (Fig. 2) absorb more efficiently, so the induction times observed for them are much shorter than for derivatives with short D–π-A. Additionally, the differences in **7M-P**, **7,8M-P**, **7,8ED-P**, and **7M-8Me-P** activity result from their polychromatic light absorption properties (I_a) and Φ_{acid}. The two most active salts are **7M-P** and **7,8ED-P**, but **7M-P** is more active at 365 nm, while **7,8ED-P** shows better activity at 405 nm. The effect is caused by nearly two times higher absorption of **7,8ED-P** in this region, whereas the Φ_{acid} is only slightly lower than that of **7M-P**.

Similar activity is observed for TEGDVE monomers. In the case of this more active monomer, coumarin salts exhibit photoinitiating activity even under VIS-LED@415 nm irradiation. Using light in the ultraviolet range, all coumarin derivatives show high photoinitiation efficiency (Fig. 6 and Table 3). During cationic photopolymerization initiated with LED@405 nm, the coumarin derivatives **5,7M-P** and **5Me-7M-P** show worse initiation properties than the other coumarin what is caused by a shorter D–π-A structure and weaker push–pull effect, as previously reported. However, in the case of the TEGDVE monomer, salt **7M-P** exhibits the best photoinitiating activity and the polymerized irradiated samples exhibit the quickest of all iodonium salts.

The photoinitiating activity of coumarin chromophore **7M** was investigated in the two-component photoinitiating system

Table 3 Coumarin based iodonium salt photoinitiating activity parameters of TEGDVE polymerization

	LED@365nm[a]			LED@405nm[b]			LED@415nm[c]		
Iodonium salt	FC [%]	τ_{ind} [s]	dC/dt	FC [%]	τ_{ind} [s]	dC/dt	FC [%]	τ_{ind} [s]	dC/dt
IOD	—	—	—	—	—	—	—	—	—
7M-P	95	1.15	8.72	95	6.52	6.18	89	4.82	0.42
7,8M-P	95	8.56	4.62	80	29.82	0.16	64	57.20	0.18
7,8ED-P	94	6.26	4.15	92	56.07	0.54	93	2.58	1.22
7M-8Me-P	97	1.94	4.94	82	26.23	0.54	71	21.86	0.17
5,7M-P	82	13.47	0.74	28	120.58	0.07	—	—	—
5Me-7M-P	71	20.49	0.32	11	136.21	0.03	—	—	—

[a] I_0 = 1.51 mW cm^{-2}. [b] I_0 = 1.47 mW cm^{-2}. [c] I_0 = 7.29 mW cm^{-2}. FC – final conversion. τ_{ind} – induction time.

Table 4 The photoinitiation efficiency of the examined coumarin photoinitiators determined by photo-DSC

	λ = 365 nm			λ = 405 nm		
Iodonium salt	Conversion [%]	R_p [mol dm^{-3} s^{-1}]	Heat flow [W g^{-1}]	Conversion [%]	R_p [mol dm^{-3} s^{-1}]	Heat flow [W g^{-1}]
OXT-221						
IOD	46.50	0.05	6.32	1.40	0	0.55
7M-P	75.70	0.15	18.20	50.30	0.10	12.82
7,8M-P	81.80	0.13	16.52	46.70	0.10	12.63
7,8ED-P	81.40	0.14	17.77	52.50	0.09	11.55
7M-8Me-P	74.50	0.13	16.22	46.30	0.03	5.20
5,7M-P	62.20	0.32	36.86	37.90	0.07	8.67
5Me-7M-P	43.10	0.04	6.40	0.30	0	0.86
BADGE						
IOD	21.10	0.11	8.66	20.70	0.01	0.68
7M-P	85.90	0.10	9.81	84.60	0.18	13.58
7,8M-P	81.90	0.09	9.06	90.30	0.11	9.24
7,8ED-P	88.80	0.10	10.21	91.20	0.14	11.48
7M-8Me-P	77.90	0.08	8.34	79.20	0.15	11.78
5,7M-P	92.00	0.16	13.80	88.00	0.18	14.00
5Me-7M-P	79.10	0.16	13.90	70.50	0.09	7.40

with **HIP** iodonium salt and compared with **7M-P** photoactivity (Fig. S35†). The obtained results show that coumarin chromophore **7M** has negligible photoactivity toward the TEGDVE monomer (toward the CADE monomer it shows no activity) compared to **7M-P** under LED@365 nm and LED@405 nm exposure. Thus, the coumarin chromophores are responsible for the high photoactivity of the presented photoinitiators but only in the form of iodonium salts.

Photo-DSC measurements

The photoinitiating activity of coumarin-based iodonium salt toward less active monomers OXT-221 and BADGE was investigated using Photo Differential Scanning Calorimetry. The activity of salts was evaluated in terms of the monomer conversion rate, the rate of the photopolymerization process Rp, and heat flow (Table 4). Graphs representing oxetane and glycidyl monomer conversions, R_p, and heat flow for each of the measurements performed are presented in the ESI (Fig. S79–S96†).

Table 5 Thermal stability of coumarin iodonium salts and their thermal activity toward TEGDVE

Iodonium salt	Thermal decomposition [°C]	Initial reaction temperature [°C]	Heat [J g^{-1}]
7M-P	167.5	62.80	532.40
7,8M-P	162.3	58.40	526.70
7,8ED-P	169.0	47.70	524.80
7M-8Me-P	152.9	54.90	547.50
5,7M-P	150.6	56.70	491.80
5Me-7M-P	—	55.30	552.70

During the process of cationic photopolymerization of the OXT-221 monomer with the application of a diode in the UV range (λ_{max} = 365 nm), it can be observed that the photoinitiators **7,8M-P**, **7,8ED-P** and **7M-P** exhibit the most favourable photoinitiating properties, while in visible light the best properties are shown by compound **7.8ED-P**, while **5Me-7M-P** does not show suitability for initiating the photopolymerization process of the OXT monomer using LED@405 nm. The obtained results follow previous information and with the characterized photochemical properties of the described salts. However, photo-DSC measurements indicate clearly that more donating groups in the coumarin chromophore lead to higher photoactivity – for longer push–pull derivatives. The one interesting exception is **5,7M-P** which can efficiently show photoinitiated polymerization of oxetane and at 365 nm it is the best quickest one. This result will be further investigated, but hypothetically the coumarin structure interacts with the secondary oxonium ion preventing the formation of the hydrogen bond and lowering the activation energy of polymerization.[76]

The photo-DSC measurements of BADGE glycidyl monomer conversions are very high for all compositions examined under ultraviolet and visible light (Table 4). Due to the high viscosity and lower reactivity of this monomer, measurements were performed at 60 °C. Under such conditions, coumarin-based iodonium salts began to behave differently than at room temperature. Glycidyl ethers like BADGE are known to be even less reactive than oxetanes.[77] However, lower reactive derivatives **5,7M-P** and **5Me-7M-P** exhibit significantly higher reactivity at elevated temperatures. What is even more interesting, at 405 nm where coumarin salts absorb less light, the reactivity is still very high (no decrease in R_p was observed). These results

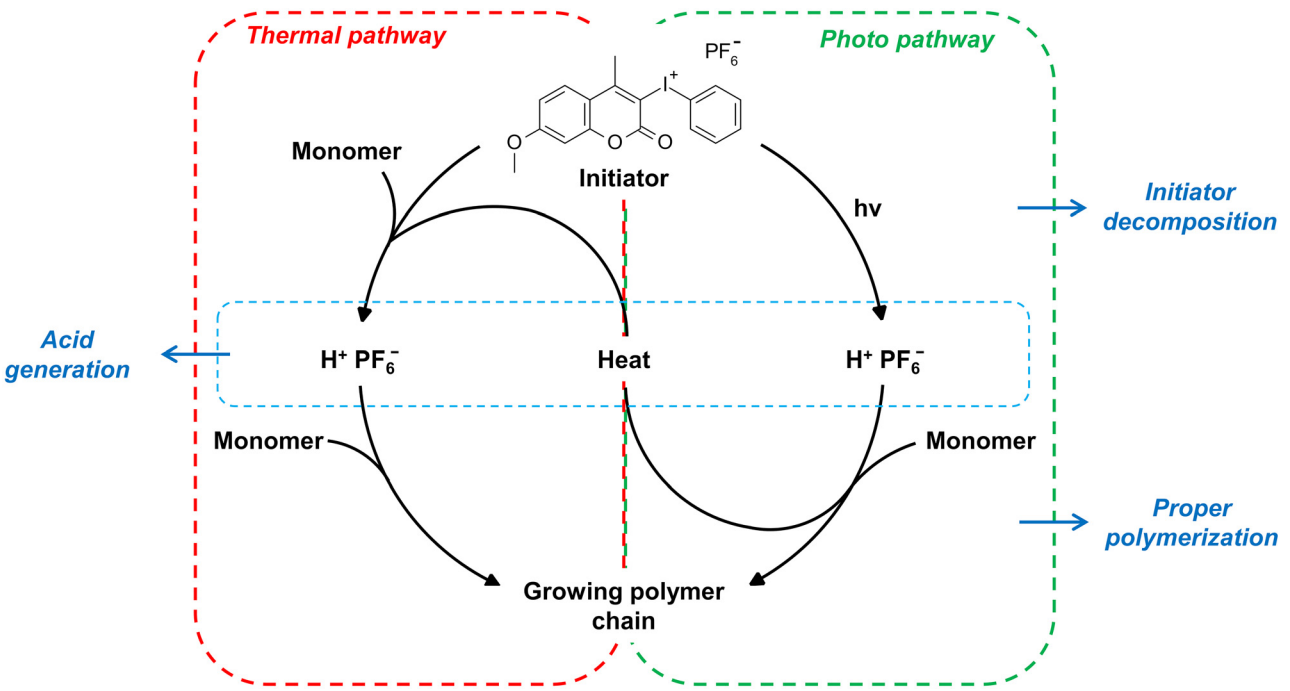

Fig. 7 Proposed mechanism of cationic polymerization initiation by coumarin based iodonium salts with two pathways of acid generation.

indicated that some iodonium salts could be significantly more active at higher temperatures. In order to investigate the thermal activity toward the cationic monomer itself, we decided to perform DSC measurements.

DSC measurements

The thermal activity of coumarin-based iodonium salts was investigated in thermal DSC measurements. They were divided into two stages. The first was to analyze the neat iodonium salt (powder) at an elevated temperature to check the decomposition temperature of the iodonium salts or to verify whether physical transformations occur in the measurement system when the salts are heated to 200 °C. The obtained DSC curves are presented in the ESI (Fig. S66–S71†).

The obtained results show that all coumarin-based iodonium salts are stable up to 150 °C (**5,7M-P**), and derivative **5Me-7M-P** is stable above 200 °C (Table 5). These results indicate that the presented new salts are stable and cannot release acid molecules in an undesirable non-specific way.

The second stage of thermal research was heating the compositions of the 1.0 wt% coumarin derivatives and TEGDVE to 120 °C (vinyl ether monomer was chosen due to its high reactivity). During the elevation of temperature, the exothermic reaction was observed (Fig. S72–S78†). In this system, such heat flow is characteristic of the polymerization reaction.

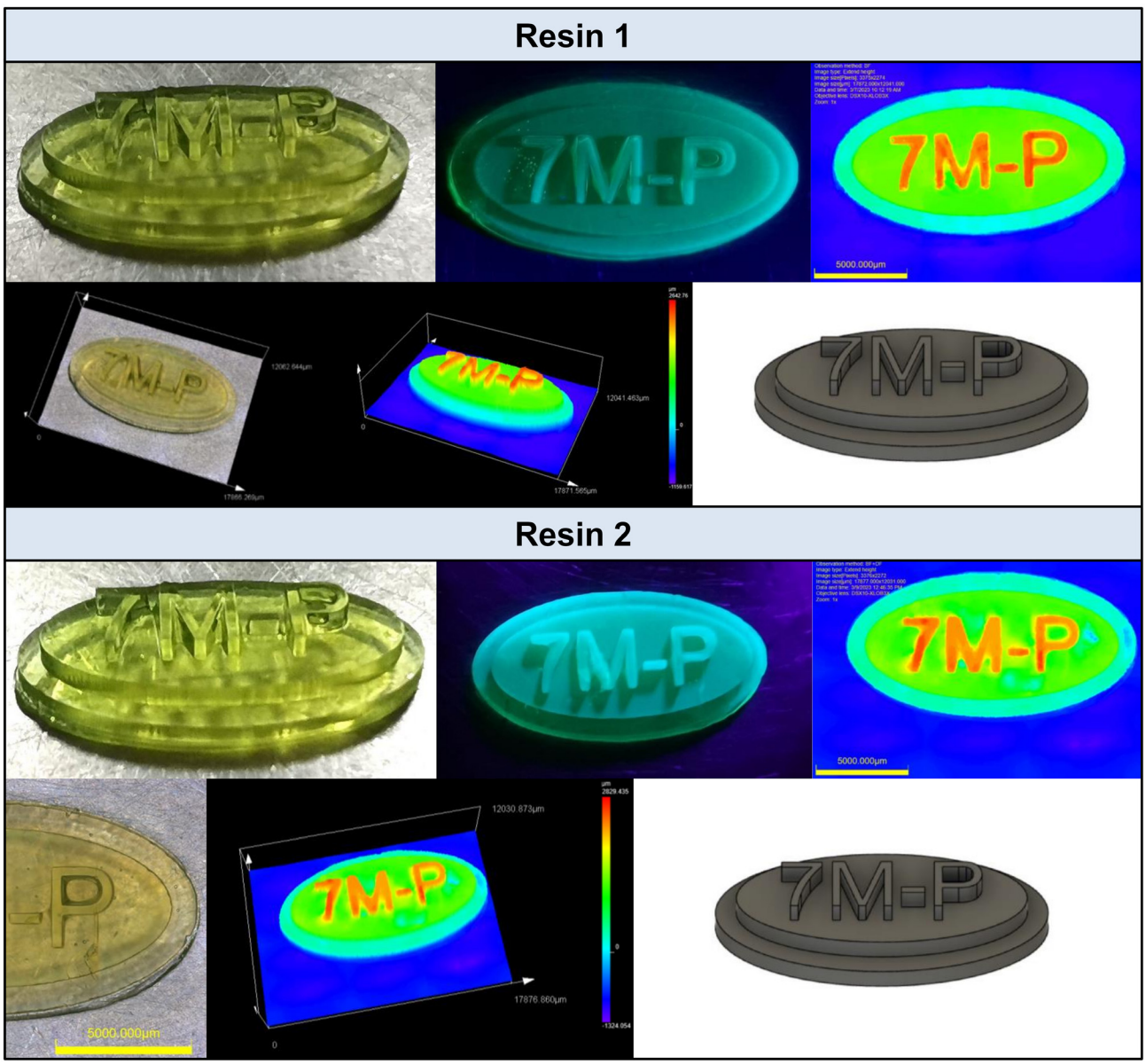

Fig. 8 Photographs of prints obtained from resins 1 and 2. Respectively from upper left to bottom right: photo taken with a phone camera in daylight; photo taken with a phone camera using a UV flashlight; three photos taken with an OLYMPUS DSX1000 optical microscope; a 3D model used for the printing process.

However, the most interesting is the initial temperature of this process (Table 5). All coumarin salts initiate polymerization in the 48–63 °C range of temperature. Such temperatures are significantly below the temperature of the thermal decomposition of these salts (about 150 °C). These results suggest that the thermal interaction must occur between monomer molecules and iodonium salts, which leads to the release of superacids. In conclusion, a non-photo acid generation pathway was discovered. Hypothetically, a substitution reaction must occur in the investigated system. This hypothesis is supported by the fact that the phenyliodonium substituent is known as the "hyper-leaving" group[78] and can undergo substitution even by weak nucleophiles (most cationic monomers).

Based on the presented results, we suggest two pathways of decomposition of coumarin iodonium salts and acid generation (Fig. 7). Thus, coumarin salts are photo-thermal initiators of cationic polymerization. Their increased reactivity at elevated temperatures can lead to better curing high scattering and opaque materials like composites and nanocomposites. Undesirable effects such as scattering and shadowing can be overcome by such new photo-thermal initiators, leading to higher conversion of monomers and better mechanical properties of cured materials.

3D-VAT printing application experiment

The final stage of the research was the development of photocurable resins, which were utilized to formulate polymer composites by additive manufacturing with Digital Light Processing (DLP) technology. **7M-P** was chosen as the photoinitiator because of its high reactivity. The prepared resin formulations contained the following components: (1) 2.0 wt% **7M-P** and CADE/OXT-221/TEGDVE (4/3/3 w/w/w); (2) 2.0 wt% **7M-P** and NANOPOX A 611/OXT-221/TEGDVE (4/3/3 w/w/w). The experiments began with measurements of the kinetics of the photopolymerization process of resins 1 and 2. During the process, the bands characteristic of the epoxy (790 cm^{-1}), oxetane (980 cm^{-1}), and vinyl (1640 cm^{-1}) groups were monitored. The measurements were carried out under aerobic conditions on a pastille made of BaF_2. Kinetic profiles and example FT-IR spectra before and after the photopolymerization process are included in the ESI (Fig. S97 and S98†). The monomer conversions for resin 1 and 2 are shown in Table S2.†

Successively, the critical energy and depth of light penetration were determined. Determination of printing parameters consisted of printing 6 slices of 1 × 1 cm by exposing the resin to a differential light for 30 s, 40 s, 60 s, 100 s, 120 s, and 150 s. Subsequently, the thickness of the cured resin layers (C_d – cured resin thickness) was measured using a micrometer screw. Based on the curing time and the power of the printing device, the energy E_0 was determined. The value of the critical energy was determined based on the intersection point with the X-axis ($C_d = f(E_0)$). Subsequently, from the prepared photo-curable resins, attempts were made to obtain polymer composites using light-initiated 3D printing technology. The 3D-VAT printing parameters and conditions are shown in Table S3.†

3D printing experiments showed that the used salt **7M-P** shows utility for 3D-VAT printing of polymer nanocomposites. The obtained prints have high resolution (Fig. 8 and Fig. S100†). For both resins 1 and 2 (without and with nanoparticles), the resolution is similar. Thus, negative effects of filler like scattering and shadowing have no significant impact on printing process initiating by coumarin based iodonium salts. This is the evidence that the photo-thermal character of new iodonium photoinitiators can overcome the drawback of photocuring of composites. Fig. S101 which facilitates comparison of the print resolution for both resins is included in the ESI.†

Therefore, coumarin based iodonium salts, especially with a longer D–π-A structure, are perfect as photoinitiators for epoxy 3D-VAT printing as well as for nanocomposite 3D-VAT printing.

Conclusion

In conclusion, the presented new iodonium salts are equipped with extended coumarin chromophores. The chromophore structure was modified with additional electron-donating substituents at positions 5 and 8. Such substitution led to a longer D–π-A structure (when the phenyliodonium group is located at position 3 and increase the polarization of the molecule) or a shorter one with hypervalent iodine located at 8 position (lower polarized D–π-A structure). Such modifications have a crucial impact on the spectral properties and photodecomposition process; derivatives with a longer D–π-A structure absorb at significantly longer wavelengths and can be photobleached during photopolymerization. However, with strengthening of the push–pull effect, the quantum yield of photoacid generation decreases.

Nevertheless, new coumarin based iodonium salts exhibit high photoinitiating activity even under LED@415 nm irradiation. They are able to photoinitiate the cationic polymerization of low reactive monomers like oxetanes and glycidyl ethers. Their photoinitiating activity is even higher at elevated temperature. This phenomenon was investigated using DSC measurements. The results indicate that coumarin iodonium salts can interact with rich-electron monomers at higher temperature with the release of an acid. This leads to a conclusion that two, photo and thermal, pathways of new iodonium salt decomposition occur in samples photoinitiated with coumarin salts.

Such behaviour of new photoinitiators can overcome the drawback of composite photocuring and eliminate problems with scattering and shadowing. This advantage of new salts was proved in DLP 3D-VAT printing of the nanocomposite. The printed patterns have high resolution regardless of whether they were obtained from a neat composition or one containing nanoadditives (the presence of nanoparticles did not disturb the printing process).

Conflicts of interest

The authors declare that they have no known competing financial interests or personal relationships that could have appeared to influence the work reported in this paper.

Acknowledgements

The presented work was funded by the OPUS LAP project contract number 2020/39/I/ST5/03556 "Advanced photopolymerized nanocomposite materials processed by additive manufacturing".

References

1 Ł. Kielesiński, O. W. Morawski, C. A. Barboza and D. T. Gryko, Polarized Helical Coumarins: [1,5] Sigmatropic Rearrangement and Excited-State Intramolecular Proton Transfer, *J. Org. Chem.*, 2021, **86**(9), 6148–6159, DOI: 10.1021/ACS.JOC.0C02978/ASSET/IMAGES/LARGE/JO0C02978_0006.JPEG.

2 O. W. Morawski, Ł. Kielesiński, D. T. Gryko and A. L. Sobolewski, Highly Polarized Coumarin Derivatives Revisited: Solvent-Controlled Competition Between Proton-Coupled Electron Transfer and Twisted Intramolecular Charge Transfer, *Chem. – Eur. J.*, 2020, **26**(32), 7281–7291, DOI: 10.1002/CHEM.202001079.

3 M. Vellakkaran and S. Hong, Visible-Light-Induced Reactions Driven by Photochemical Activity of Quinolinone and Coumarin Scaffolds, *Asian J. Org. Chem.*, 2021, **10**(5), 1012–1023, DOI: 10.1002/AJOC.202100162.

4 M. Stojanović, N. Flores-Diaz, Y. Ren, N. Vlachopoulos, L. Pfeifer, Z. Shen, Y. Liu, S. M. Zakeeruddin, J. V. Milić and A. Hagfeldt, The Rise of Dye-Sensitized Solar Cells: From Molecular Photovoltaics to Emerging Solid-State Photovoltaic Technologies, *Helv. Chim. Acta*, 2021, **104**(4), e2000230, DOI: 10.1002/HLCA.202000230.

5 K. V. Basavarajappa, Y. Arthoba Nayaka, H. T. Purushothama, M. M. Vinaya, A. Antony and P. Poornesh, Optoelectronic and Current-Voltage Studies for Novel Coumarin Dyes, *Int. J. Environ. Anal. Chem.*, 2019, **101**(1), 113–126, DOI: 10.1080/03067319.2019.1661395.

6 A. Kumar, R. Baccoli, A. Fais, A. Cincotti, L. Pilia and G. Gatto, Substitution Effects on the Optoelectronic Properties of Coumarin Derivatives, *Appl. Sci.*, 2019, **10**(1), 144, DOI: 10.3390/APP10010144.

7 E. Kim and S. B. Park, Chemistry as a Prism: A Review of Light-Emitting Materials Having Tunable Emission Wavelengths, *Chem. – Asian J.*, 2009, **4**(11), 1646–1658, DOI: 10.1002/ASIA.200900102.

8 J. Ortyl, M. Topa, I. Kamińska-Borek and R. Popielarz, Mechanism of Interaction of Aminocoumarins with Reaction Medium during Cationic Photopolymerization of Triethylene Glycol Divinyl Ether, *Eur. Polym. J.*, 2019, **116**, 45–55, DOI: 10.1016/J.EURPOLYMJ.2019.03.060.

9 I. Kamińska, J. Ortyl and R. Popielarz, Mechanism of Interaction of Coumarin-Based Fluorescent Molecular Probes with Polymerizing Medium during Free Radical Polymerization of a Monomer, *Polym. Test.*, 2016, **55**, 310–317, DOI: 10.1016/J.POLYMERTESTING.2016.09.013.

10 I. Kamińska, J. Ortyl and R. Popielarz, Applicability of Quinolizino-Coumarins for Monitoring Free Radical Photopolymerization by Fluorescence Spectroscopy, *Polym. Test.*, 2015, **42**, 99–107, DOI: 10.1016/J.POLYMERTESTING.2014.12.013.

11 J. Ortyl and R. Popielarz, The Performance of 7-Hydroxycoumarin-3-Carbonitrile and 7-Hydroxycoumarin-3-Carboxylic Acid as Fluorescent Probes for Monitoring of Cationic Photopolymerization Processes by FPT, *J. Appl. Polym. Sci.*, 2013, **128**(3), 1974–1978, DOI: 10.1002/app.38378.

12 J. Ortyl, K. Sawicz and R. Popielarz, Performance of Amidocoumarins as Probes for Monitoring of Cationic Photopolymerization of Monomers by Fluorescence Probe Technology, *J. Polym. Sci., Part A: Polym. Chem.*, 2010, **48**(20), 4522–4528, DOI: 10.1002/POLA.24243.

13 L. M. Wysocki and L. D. Lavis, Advances in the Chemistry of Small Molecule Fluorescent Probes, *Curr. Opin. Chem. Biol.*, 2011, **15**(6), 752–759, DOI: 10.1016/J.CBPA.2011.10.013.

14 Q. Chen, Q. Yang, P. Gao, B. Chi, J. Nie and Y. He, Photopolymerization of Coumarin-Containing Reversible Photoresponsive Materials Based on Wavelength Selectivity, *Ind. Eng. Chem. Res.*, 2019, **58**(8), 2970–2975, DOI: 10.1021/ACS.IECR.8B05164/SUPPL_FILE/IE8B05164_SI_001.PDF.

15 K. Górski, I. Deperasińska, G. V. Baryshnikov, S. Ozaki, K. Kamada, H. Ågren and D. T. Gryko, Quadrupolar Dyes Based on Highly Polarized Coumarins, *Org. Lett.*, 2021, **23**(17), 6770–6774, DOI: 10.1021/ACS.ORGLETT.1C02349/ASSET/IMAGES/LARGE/OL1C02349_0004.JPEG.

16 F. Dumur, Recent Advances on Coumarin-Based Photoinitiators of Polymerization, *Eur. Polym. J.*, 2022, **163**, 110962, DOI: 10.1016/J.EURPOLYMJ.2021.110962.

17 M. Abdallah, A. Hijazi, F. Dumur and J. Lalevée, Coumarins as Powerful Photosensitizers for the Cationic Polymerization of Epoxy-Silicones under Near-UV and Visible Light and Applications for 3D Printing Technology, *Molecules*, 2020, **25**(9), 2063, DOI: 10.3390/MOLECULES25092063.

18 B. Kiskan and Y. Yagci, Self-Healing of Poly(Propylene Oxide)-Polybenzoxazine Thermosets by Photoinduced Coumarine Dimerization, *J. Polym. Sci., Part A: Polym. Chem.*, 2014, **52**(20), 2911–2918, DOI: 10.1002/POLA.27323.

19 M. B. Sims, B. Zhang, Z. M. Gdowski, T. P. Lodge and F. S. Bates, Nondestructive Photo-Cross-Linking of Microphase-Separated Diblock Polymers through Coumarin Dimerization, *Macromolecules*, 2022, **55**(8), 3317–3324, DOI: 10.1021/ACS.MACROMOL.2C00356/SUPPL_FILE/MA2C00356_SI_001.PDF.

20 Y. J. Eng, J. Xu, S. Sugiarto, U. S. Jonnalagadda, W. Ang, J. H. C. Lee, J. J. Kwan and T. M. Nguyen, Initiator-Free Photohydrogelation of Linear Coumarin-Containing Poly (Ethylene Glycol) Methacrylates and Study of Ultrasound-Triggered Gel Breakdown, *ACS Appl. Polym. Mater.*, 2021, **3**(8), 4264–4274, DOI: **10.1021/ACSAPM.1C00752/SUPPL_FILE/AP1C00752_SI_001.PDF**.

21 J. P. Chesterman, T. C. Hughes and B. G. Amsden, Reversibly Photo-Crosslinkable Aliphatic Polycarbonates Functionalized with Coumarin, *Eur. Polym. J.*, 2018, **105**, 186–193, DOI: **10.1016/J.EURPOLYMJ.2018.05.038**.

22 F. Zhang, L. Zhu, Z. Li, S. Wang, J. Shi, W. Tang, N. Li and J. Yang, The Recent Development of Vat Photopolymerization: A Review, *Addit. Manuf.*, 2021, **48**, 102423, DOI: **10.1016/J.ADDMA.2021.102423**.

23 S. C. Ligon, R. Liska, J. Stampfl, M. Gurr and R. Mülhaupt, Polymers for 3D Printing and Customized Additive Manufacturing, *Chem. Rev.*, 2017, **117**(15), 10212–10290, DOI: **10.1021/acs.chemrev.7b00074**.

24 Z. Faraji Rad, P. D. Prewett and G. J. Davies, High-Resolution Two-Photon Polymerization: The Most Versatile Technique for the Fabrication of Microneedle Arrays, *Microsyst. Nanoeng.*, 2021, **7**(1), 1–17, DOI: **10.1038/s41378-021-00298-3**.

25 X. Jing, H. Fu, B. Yu, M. Sun and L. Wang, Two-Photon Polymerization for 3D Biomedical Scaffolds: Overview and Updates, *Front. Bioeng. Biotechnol.*, 2022, **10**, 994355, DOI: **10.3389/FBIOE.2022.994355**.

26 B. A. Suslick, J. Hemmer, B. R. Groce, K. J. Stawiasz, P. H. Geubelle, G. Malucelli, A. Mariani, J. S. Moore, J. A. Pojman and N. R. Sottos, Frontal Polymerizations: From Chemical Perspectives to Macroscopic Properties and Applications, *Chem. Rev.*, 2023, **123**(6), 3237–3298, DOI: **10.1021/ACS.CHEMREV.2C00686**.

27 Q. Li, H. X. Shen, C. Liu, C. F. Wang, L. Zhu and S. Chen, Advances in Frontal Polymerization Strategy: From Fundamentals to Applications, *Prog. Polym. Sci.*, 2022, **127**, 101514, DOI: **10.1016/J.PROGPOLYMSCI.2022.101514**.

28 F. Petko, A. Świeży and J. Ortyl, Photoinitiating Systems and Kinetics of Frontal Photopolymerization Processes – the Prospects for Efficient Preparation of Composites and Thick 3D Structures, *Polym. Chem.*, 2021, **12**(32), 4593–4612, DOI: **10.1039/D1PY00596K**.

29 J. V. Crivello, Photopolymerization, in *Polymer Science: A Comprehensive Reference*, Elsevier, 2012, Vol. 4, pp. 919–955. DOI: **10.1016/B978-0-444-53349-4.00123-0**.

30 F. Dumur, Recent Advances on Photobleachable Visible Light Photoinitiators of Polymerization, *Eur. Polym. J.*, 2023, **186**, 111874, DOI: **10.1016/J.EURPOLYMJ.2023.111874**.

31 M. Rahal, B. Graff, J. Toufaily, T. Hamieh, F. Dumur and J. Lalevée, Design of Keto-Coumarin Based Photoinitiator for Free Radical Photopolymerization: Towards 3D Printing and Photocomposites Applications, *Eur. Polym. J.*, 2021, **154**, 110559, DOI: **10.1016/J.EURPOLYMJ.2021.110559**.

32 Z. Liu and F. Dumur, Recent Advances on Visible Light Coumarin-Based Oxime Esters as Initiators of Polymerization, *Eur. Polym. J.*, 2022, **177**, 111449, DOI: **10.1016/J.EURPOLYMJ.2022.111449**.

33 F. Hammoud, N. Giacoletto, G. Noirbent, B. Graff, A. Hijazi, M. Nechab, D. Gigmes, F. Dumur and J. Lalevée, Substituent Effects on the Photoinitiation Ability of Coumarin-Based Oxime-Ester Photoinitiators for Free Radical Photopolymerization, *Mater. Chem. Front.*, 2021, **5**(24), 8361–8370, DOI: **10.1039/D1QM01310F**.

34 X. Zhao, Y. Zhao, M. D. Li, Z. Li, H. Peng, T. Xie and X. Xie, Efficient 3D Printing via Photooxidation of Ketocoumarin Based Photopolymerization, *Nat. Commun.*, 2021, **12**(1), 1–8, DOI: **10.1038/s41467-021-23170-4**.

35 S. Fan, X. Sun, X. He, Y. Pang, Y. Xin, Y. Ding and Y. Zou, Coumarin Ketoxime Ester with Electron-Donating Substituents as Photoinitiators and Photosensitizers for Photopolymerization upon UV-Vis LED Irradiation, *Polymers*, 2022, **14**(21), 4588, DOI: **10.3390/POLYM14214588/S1**.

36 Z. Li, X. Zou, G. Zhu, X. Liu and R. Liu, Coumarin-Based Oxime Esters: Photobleachable and Versatile Unimolecular Initiators for Acrylate and Thiol-Based Click Photopolymerization under Visible Light-Emitting Diode Light Irradiation, *ACS Appl. Mater. Interfaces*, 2018, **10**(18), 16113–16123, DOI: **10.1021/ACSAMI.8B01767/SUPPL_FILE/AM8B01767_SI_001.PDF**.

37 M. Li, J. Zhu, P. Hu, Z. Li and R. Liu, Synthesis and Properties of Coumarin-Based Alicyclic Oxime-Esters as Visible Light Photoinitiators, *Imaging Sci. Photochem.*, 2022, **40**(4), 704, DOI: **10.7517/ISSN.1674-0475.220205**.

38 N. Guy, O. Giani, S. Blanquer, J. Pinaud and J. J. Robin, Photoinduced Ring-Opening Polymerizations, *Prog. Org. Coat.*, 2021, **153**, 106159, DOI: **10.1016/J.PORGCOAT.2021.106159**.

39 K. Kaya, H. C. Kiliclar and Y. Yagci, Photochemically Generated Ionic Species for Cationic and Step-Growth Polymerizations, *Eur. Polym. J.*, 2023, **190**, 112000, DOI: **10.1016/J.EURPOLYMJ.2023.112000**.

40 P. Xiao, J. Zhang, F. Dumur, M. A. Tehfe, F. Morlet-Savary, B. Graff, D. Gigmes, J. P. Fouassier and J. Lalevée, Visible Light Sensitive Photoinitiating Systems: Recent Progress in Cationic and Radical Photopolymerization Reactions under Soft Conditions, *Prog. Polym. Sci.*, 2015, **41**(C), 32–66, DOI: **10.1016/J.PROGPOLYMSCI.2014.09.001**.

41 Z. Yang, J. Chen and S. Liao, Monophosphoniums as Effective Photoredox Organocatalysts for Visible Light-Regulated Cationic RAFT Polymerization, *ACS Macro Lett.*, 2022, **11**(9), 1073–1078, DOI: **10.1021/ACSMACROLETT.2C00418/SUPPL_FILE/MZ2C00418_SI_001.PDF**.

42 Y. Y. Durmaz, Ö. Zaim and Y. Yagci, Diethoxy-Azobis (Pyridinium) Salt as Photoinitiator for Cationic Polymerization: Towards Wavelength Tunability by Cis–Trans Isomerization, *Macromol. Rapid Commun.*, 2008, **29**(11), 892–896, DOI: **10.1002/MARC.200800070**.

43 S. Chen, C. Cao, X. Shen, Y. Qiu, C. Kuang, D. Wan and M. Jin, One/Two-Photon Sensitive Sulfonium Salt Photoinitiators Based on 1,3,5-Triphenyl-2-Pyrazoline, *Eur. Polym. J.*, 2021, **153**, 110525, DOI: **10.1016/J.EURPOLYMJ.2021.110525**.

44 M. Sangermano, N. Razza and J. V. Crivello, Cationic UV-Curing: Technology and Applications, *Macromol. Mater. Eng.*, 2014, **299**(7), 775–793, DOI: **10.1002/MAME.201300349**.

45 Y. Yagci, S. Jockusch and N. J. Turro, Photoinitiated Polymerization: Advances, Challenges, and Opportunities, *Macromolecules*, 2010, **43**(15), 6245–6260, DOI: **10.1021/MA1007545/ASSET/IMAGES/MEDIUM/MA-2010-007545_0001.GIF**.

46 Y. Zhu, L. Li, Y. Zhang, Y. Ou, J. Zhang, Y. Yagci and R. Liu, Broad Wavelength Sensitive Coumarin Sulfonium Salts as Photoinitiators for Cationic, Free Radical and Hybrid Photopolymerizations, *Prog. Org. Coat.*, 2023, **174**, 107272, DOI: **10.1016/J.PORGCOAT.2022.107272**.

47 L. Li, J. Zhang, J. Luo, R. Liu and Y. Zhu, Synthesis and Properties of UV/Vis-LED Excitable Photoinitiators Based on Coumarin Pyridinium Salt, *Chem. J. Chin. Univ.*, 2022, **43**(10), 20220178, DOI: **10.7503/CJCU20220178**.

48 L. Li, M. Wan, Z. Li, Y. Luo, S. Wu, X. Liu and Y. Yagci, Coumarinacyl Anilinium Salt: A Versatile Visible and NIR Photoinitiator for Cationic and Step-Growth Polymerizations, *ACS Macro Lett.*, 2023, 263–268, DOI: **10.1021/ACSMACROLETT.2C00675/SUPPL_FILE/MZ2C00675_SI_001.PDF**.

49 P. Pröhm, W. Berg, S. M. Rupf, C. Müller and S. Riedel, On Pyridine Chloronium Cations, *Chem. Sci.*, 2023, **14**(9), 2325–2329, DOI: **10.1039/D2SC06757A**.

50 J. V. Crivello and J. H. W. Lam, Diaryliodonium Salts. A New Class of Photoinitiators for Cationic Polymerization, *Macromolecules*, 1977, **10**(6), 1307–1315, DOI: **10.1021/ma60060a028**.

51 J. V. Crivello and J. L. Lee, Alkoxy-Substituted Diaryliodonium Salt Cationic Photoinitiators, *J. Polym. Sci., Part A: Polym. Chem.*, 1989, **27**(12), 3951–3968, DOI: **10.1002/POLA.1989.080271207**.

52 C. Dietlin, S. Schweizer, P. Xiao, J. Zhang, F. Morlet-Savary, B. Graff, J. P. Fouassier and J. Lalevée, Photopolymerization upon LEDs: New Photoinitiating Systems and Strategies, *Polym. Chem.*, 2015, **6**(21), 3895–3912, DOI: **10.1039/C5PY00258C**.

53 E. Merritt and B. Olofsson, Diaryliodonium Salts: A Journey from Obscurity to Fame, *Angew. Chem., Int. Ed.*, 2009, **48**(48), 9052–9070, DOI: **10.1002/anie.200904689**.

54 S. Villotte, D. Gigmes, F. Dumur and J. Lalevée, Design of Iodonium Salts for UV or Near-UV LEDs for Photoacid Generator and Polymerization Purposes, *Molecules*, 2019, **25**(1), 149, DOI: **10.3390/molecules25010149**.

55 N. Zivic, M. Bouzrati-Zerrelli, S. Villotte, F. Morlet-Savary, C. Dietlin, F. Dumur, D. Gigmes, J. P. Fouassier and J. Lalevée, A Novel Naphthalimide Scaffold Based Iodonium Salt as a One-Component Photoacid/Photoinitiator for Cationic and Radical Polymerization under LED Exposure, *Polym. Chem.*, 2016, **7**(37), 5873–5879, DOI: **10.1039/c6py01306f**.

56 F. Petko, M. Galek, E. Hola, R. Popielarz and J. Ortyl, One-Component Cationic Photoinitiators from Tunable Benzylidene Scaffolds for 3D Printing Applications, *Macromolecules*, 2021, **54**(15), 7070–7087, DOI: **10.1021/ACS.MACROMOL.1C01048/SUPPL_FILE/MA1C01048_SI_001.PDF**.

57 F. Petko, M. Galek, E. Hola, M. Topa-Skwarczyńska, W. Tomal, M. Jankowska, M. Pilch, R. Popielarz, B. Graff, F. Morlet-Savary, J. Lalevee and J. Ortyl, Symmetric Iodonium Salts Based on Benzylidene as One-Component Photoinitiators for Applications in 3D Printing, *Chem. Mater.*, 2022, **2022**, 10077–10092, DOI: **10.1021/ACS.CHEMMATER.2C02796**.

58 M. Topa-Skwarczyńska, M. Galek, M. Jankowska, F. Morlet-Savary, B. Graff, J. Lalevée, R. Popielarz and J. Ortyl, Development of the First Panchromatic BODIPY-Based One-Component Iodonium Salts for Initiating the Photopolymerization Processes, *Polym. Chem.*, 2021, **12**(47), 6873–6893, DOI: **10.1039/D1PY01263K**.

59 X. Peng, M. Yao and P. Xiao, Newly Synthesized Chromophore-Linked Iodonium Salts as Photoinitiators of Free Radical Photopolymerization, *Macromol. Chem. Phys.*, 2021, **222**(9), 2100035, DOI: **10.1002/MACP.202100035**.

60 J. Ortyl and R. Popielarz, New Photoinitiators for Cationic Polymerization, *Polimery*, 2012, **57**(7–8), 510–517.

61 H. Mokbel, J. Toufaily, T. Hamieh, F. Dumur, D. Campolo, D. Gigmes, J. Pierre Fouassier, J. Ortyl and J. Lalevée, Specific Cationic Photoinitiators for near UV and Visible LEDs: Iodonium versus Ferrocenium Structures, *J. Appl. Polym. Sci.*, 2015, **132**(46), 42759, DOI: **10.1002/app.42759**.

62 M. Topa, E. Hola, M. Galek, F. Petko, M. Pilch, R. Popielarz, F. Morlet-Savary, B. Graff, J. Laleveé and J. Ortyl, One-Component Cationic Photoinitiators Based on Coumarin Scaffold Iodonium Salts as Highly Sensitive Photoacid Generators for 3D Printing IPN Photopolymers under Visible LED Sources, *Polym. Chem.*, 2020, **11**(32), 5261–5278, DOI: **10.1039/d0py00677g**.

63 G. Pohlers, J. C. Scaiano and R. Sinta, A Novel Photometric Method for the Determination of Photoacid Generation Efficiencies Using Benzothiazole and Xanthene Dyes as Acid Sensors, *Chem. Mater.*, 1997, **9**(12), 3222–3230, DOI: **10.1021/cm970587p**.

64 C. G. Hatchard and C. A. Parker, A New Sensitive Chemical Actinometer - II. Potassium Ferrioxalate as a Standard Chemical Actinometer, *Proc. R. Soc. London, Ser. A*, 1956, **235**(1203), 518–536, DOI: **10.1098/rspa.1956.0102**.

65 H. J. Kuhn, S. E. Braslavsky and R. Schmidt, Chemical Actinometry (IUPAC Technical Report), *Pure Appl. Chem.*, 2004, **76**(12), 2105–2146, DOI: **10.1351/PAC200476122105/MACHINEREADABLECITATION/RIS**.

66 J. Bennett, Measuring UV Curing Parameters of Commercial Photopolymers Used in Additive Manufacturing, *Addit. Manuf.*, 2017, **18**, 203–212, DOI: **10.1016/J.ADDMA.2017.10.009**.

67 W. Tomal, D. Krok, A. Chachaj-Brekiesz, P. Lepcio and J. Ortyl, Harnessing Light to Create Functional, Three-Dimensional Polymeric Materials: Multitasking Initiation Systems as the Critical Key to Success, *Addit. Manuf.*, 2021, **48**, 102447, DOI: **10.1016/J.ADDMA.2021.102447**.

68 M. Yamaji, Y. Hakoda, H. Okamoto and F. Tani, Photochemical Synthesis and Photophysical Properties of Coumarins Bearing Extended Polyaromatic Rings Studied by Emission and Transient Absorption Measurements, *Photochem. Photobiol. Sci.*, 2017, **16**(4), 555–563, DOI: **10.1039/C6PP00399K**.

69 C. Hansch, A. Leo and R. W. Taft, A Survey of Hammett Substituent Constants and Resonance and Field Parameters, *Chem. Rev.*, 1991, **91**(2), 165–195, DOI: **10.1021/cr00002a004**.

70 F. Bureš, Fundamental Aspects of Property Tuning in Push–Pull Molecules, *RSC Adv.*, 2014, **4**(102), 58826–58851, DOI: **10.1039/C4RA11264D**.

71 B. Strehmel, C. Schmitz, T. Brömme, A. Halbhuber, D. Oprych and J. S. Gutmann, Advances of near Infrared Sensitized Radical and Cationic Photopolymerization: From Graphic Industry to Traditional Coatings, *J. Photopolym. Sci. Technol.*, 2016, **29**(1), 111–121, DOI: **10.2494/photopolymer.29.111**.

72 A. Shiraishi, Y. Ueda, M. Schläpfer, C. Schmitz, T. Brömme, D. Oprych and B. Strehmel, Nir-Sensitized Photopolymerization with Iodonium Salts Bearing Weak Coordinating Anions, *J. Photopolym. Sci. Technol.*, 2016, **29**(4), 609–615, DOI: **10.2494/photopolymer.29.609**.

73 C. W. Cho, T. P. T. Pham, Y. C. Jeon and Y. S. Yun, Influence of Anions on the Toxic Effects of Ionic Liquids to a Phytoplankton Selenastrum Capricornutum, *Green Chem.*, 2008, **10**(1), 67–72, DOI: **10.1039/B705520J**.

74 Y. Yağci and I. Reetz, Externally Stimulated Initiator Systems for Cationic Polymerization, *Prog. Polym. Sci.*, 1998, **23**(8), 1485–1538, DOI: **10.1016/S0079-6700(98)00010-0**.

75 D. Bomze, P. Knaack and R. Liska, Successful Radical Induced Cationic Frontal Polymerization of Epoxy-Based Monomers by C-C Labile Compounds, *Polym. Chem.*, 2015, **6**(47), 8161–8167, DOI: **10.1039/c5py01451d**.

76 J. V. Crivello, Deslgn of Photoacid Generatlng Systems, *J. Photopolym. Sci. Technol.*, 2009, 575–582, DOI: **10.2494/photopolymer.22.575**.

77 J. V. Crivello, Cationic Photopolymerization of Alkyl Glycidyl Ethers, *J. Polym. Sci., Part A: Polym. Chem.*, 2006, **44**(9), 3036–3052, DOI: **10.1002/pola.21419**.

78 J. Malmgren, S. Santoro, N. Jalalian, F. Himo and B. Olofsson, Arylation with Unsymmetrical Diaryliodonium Salts: A Chemoselectivity Study, *Chem. – Eur. J.*, 2013, **19**(31), 10334–10342, DOI: **10.1002/CHEM.201300860**.